

# Micro Newton Colloid Thruster System Development

Vlad Hruby, Manuel Gamero-Castaño, Paul Falkos, and Suren Shenoy  
Busek Co. Inc.  
11 Tech Circle  
Natick, MA 01760-1023  
busek@busek.com  
508-655-5565

IEPC-01-281

**A first prototype, laboratory colloid thruster system was developed and delivered to NASA JPL. It is capable of delivering continuously and broadly adjustable thrust in the range of micro Newtons while exceeding the required thrust resolution and thrust temporal stability of 0.1  $\mu$ N.**

## Abstract

A first prototype, laboratory colloid thruster system was developed and delivered to NASA JPL. It is capable of delivering continuously and broadly adjustable thrust in the range of micro Newtons while exceeding the required thrust resolution and thrust temporal stability of 0.1  $\mu$ N.

The thruster system consists of the colloid thruster itself, field emission cathode neutralizer, feed system with propellant storage and a power processor. The whole laboratory system is contained in an aluminum housing/frame that has 9x5x5 inches envelope, weighs about 2.5 kg including enough of propellant to operate at maximum thrust for approximately 3000 hours. The system is controlled from a PC with Lab View software.

The thruster has 57 individual emitters (needles) aligned with an extractor grid and an accelerator grid that are somewhat analogous to conventional ion thruster grids. The double grid facilitates a stable Taylor cone, a requirement for 0.1  $\mu$ N thrust stability, while allowing variable colloid acceleration/thrust generation.

The field emission (FE) neutralizer is based on Busek's carbon nanotube (CNT) electron emitter. The CNTFE cathode consists of the CNT emitter and a gate electrode. We have successfully demonstrated spacecraft charge/beam neutralization using the CNTFE cathode which is a first in EP propulsion.

The feed system consists of a propellant storage, micro latching valve and a pressurant system based on zeolite crystals. The propellant is stored inside stainless steel bellows and is forced out by external gas pressure generated by heating the zeolite.

The power processor consists of several commercial DC to DC converters for operating the thruster, the CNTFE cathode, the zeolite heater and the latching valve magnetics.

The paper focuses on the colloid thruster system from a global point of view, giving top-level design and performance characteristics of the subsystems while differing detailed component and performance description to companion papers presented at the same conference.

## 1.0 INTRODUCTION AND BACKGROUND

Microthruster systems capable of delivering smoothly variable thrust in the range of 1  $\mu$ N to 1 mN are required for providing primary propulsion

---

Copyright © 2001 by V. Hruby. Published by the Electric Rocket Propulsion Society with permission.  
Presented as Paper IEPC-01-281 at the 27<sup>th</sup> International Electric Propulsion Conference, Pasadena, CA, 15-19 October, 2001

for nano and microspacecraft and precise position control of individual spacecraft in a cluster of satellites in coordinated formation flight. The microthrusters capable of meeting this requirement at high efficiency (>60%) and specific impulse (>500 sec) include colloid thrusters<sup>1</sup> and FEPP thrusters<sup>2,3</sup>.

NASA missions that require precise position control are numerous and include those identified by their acronyms in Figure 1. The Laser Interferometer Space Antenna (LISA), Earth Science Experimental Mission 5 (EX-5), and Laser Interplanetary Ranging Experiment (LIRE) may require “drag-free” or similar level of precision. Drag-free operation requires that the position of the spacecraft containing a freely floating test mass be controlled with nanometer precision by continuously firing a set of microthrusters to counteract all disturbances, such as gravity anomalies and solar radiation pressure to keep the test mass centered in its housing.

Other missions shown in Figure 1 have broader propulsion requirements -  $\mu\text{N}$  thrusters for position control and some  $\text{mN}$ 's for system reconfiguration and to acquire new targets. These missions include the Terrestrial Planet Finder (TPF), the Micro-Arcsecond X-ray Interferometer Mission (MAXIM), and the Submillimeter probe of the Evolution of Cosmic structure (SPECS).

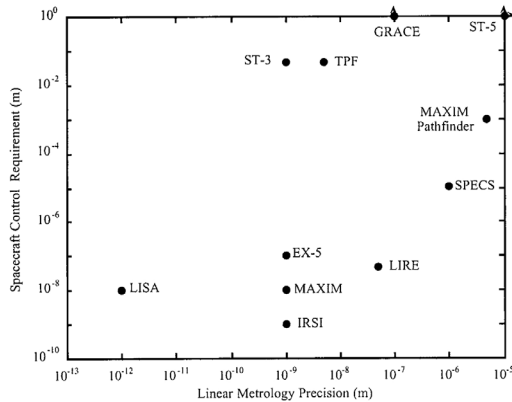


Figure 1 Spacecraft position and metrology requirements for various missions<sup>4</sup>

Busek’s micropropulsion efforts to satisfy these missions were directed at the colloid thruster since mid to late nineties. With newly available and improved understanding of the electro spray physics

Busek built on colloid thruster research initiated in the sixties and discontinued for apparently non-technical reasons in the seventies. During this later period high performance colloid thrusters with up to 70% efficiency and 1400 sec specific impulse were demonstrated in the laboratory<sup>5,6</sup> and at least one life test exceeding 4000 hours was carried out. A major impediment to achieving even better results was an insufficient level of understanding of the colloid physics, evident from the period publications, and the attendant necessity to operate the thrusters at very high voltages which resulted in heavy, bulky systems. Since then the colloid physics/electrospray science has achieved great progress due to its terrestrial applications in the chemical and biomedical fields where it is used to create and identify large molecules through electro spray mass spectrometry.<sup>7,8</sup> Capitalizing on the advances in physics, high voltage power electronics, development of new fluids suitable for colloid propellants, and on-going research sponsored by NASA Glenn Center,<sup>9,10</sup> it is now possible to develop a more compact, efficient, highly controllable colloid thruster system that operates at significantly lower voltages than those in the seventies.

## 2.0 REQUIREMENTS AND DESIGN PHILOSOPHY

The anticipated colloid propulsion mission requirements include a thrust level of the order of 1 to 100  $\mu\text{N}$  with specific impulse of the order of 500 sec. The thruster design is not sensitive to absolute requirements given that the same thruster can operate with different propellants with varying electrical conductivity thus yielding different thrust levels. High  $I_{sp}$  is not particularly important given that the anticipated micropropulsion  $\Delta V$  is low. The expressions below show thrust (T) and  $I_{sp}$  dependence on the propellant properties.

$$T \sim (2V_A \rho f(\epsilon))^{1/2} \left( \frac{K\gamma \dot{m}^3}{\epsilon \rho^3} \right)^{1/4} n \quad [1]$$

$$I_{sp} \sim \frac{1}{g} \left( \frac{2V_A f(\epsilon)}{\rho} \right)^{1/2} \left( \frac{K\rho\gamma}{\dot{m}\epsilon} \right)^{1/4} \quad [2]$$

where  $V_A$  is the acceleration voltage,  $\rho$  is propellant density,  $f(\epsilon)$  is constant factor dependant on the propellant dielectric constant  $\epsilon$ ,  $K$  is the propellant electrical conductivity and  $\gamma$  its surface tension. The quantities  $\dot{m}$  and  $n$  are the propellant mass flow per emitter needle and  $n$  is the number of needles in the thruster.  $K$  is the easiest to manipulate by additives to the basic propellant and by varying the propellant temperature. To vary thrust at a constant  $I_{sp}$  requires varying  $\dot{m}$  and  $V_A$  as

$$T|_{I_{sp}} \approx \dot{m}; \quad V_A|_{I_{sp}} \approx \sqrt{\dot{m}} \quad [3]$$

Practically any thrust level and  $I_{sp}$  can be achieved if no restrictions are placed on  $V_A$  and choice of propellants. Crucial however to the success of the missions shown in Figure 1, especially those operating in “Drag Free” mode<sup>11</sup>, is thrust resolution and temporal stability. The New Millennium Program ST7/DRS mission requires thrust resolution of 0.1  $\mu$ N in the range from 1 to 20  $\mu$ N, stable over a period of at least 1000 sec. The thrust resolution and stability requirement became the major focus of our design effort and drove many design decisions especially on the thruster itself.

The most important consequence of the 0.1  $\mu$ N stability requirement is the addition of a second electrode (accelerator) to the thruster. It accelerates the charged nano-droplets to the desired velocity while the first electrode (extractor) extracts the droplets from the Taylor cone at a nearly constant voltage. This ensures that the Taylor cone is always stable without abrupt transitions into multi-cone emission sites whose occurrence is documented in Figure 2 and Figure 3. With a stable single cone jet per needle, the thruster is stable within 0.001  $\mu$ N over a broad range of thrust<sup>1</sup>.

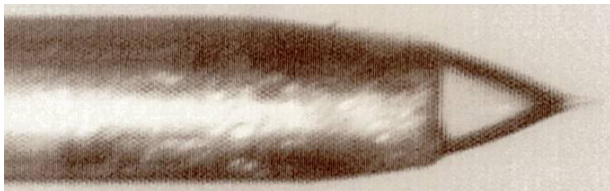


Figure 2a Cone-jet of glycerol. The needle voltage is set at 2600 V. The liquid meniscus ends in one on-axis jet

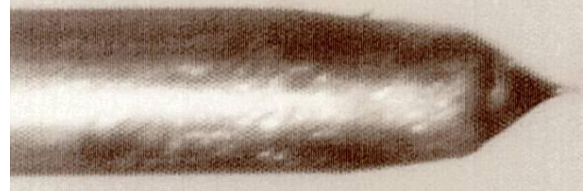


Figure 2b Cone-jet of glycerol. The needle voltage is 3230 V

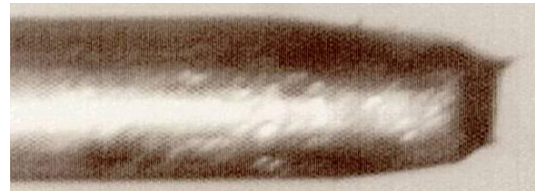


Figure 2c Glycerol in a multi-cone spraying mode. The needle voltage is set at 3600 V. Two off-axis emission points are observed

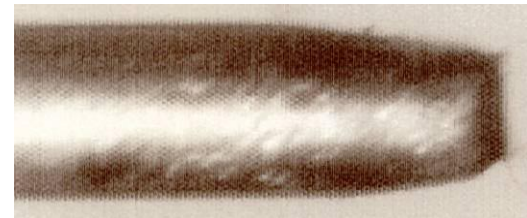


Figure 2d Glycerol in a multi-cone spraying mode.  $V_{on} = 3690$  V. Three emission points are barely spotted

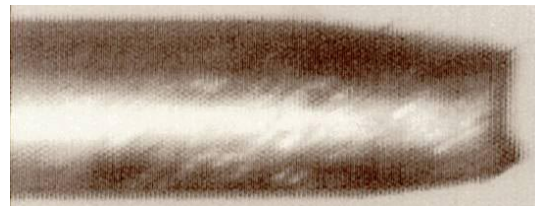


Figure 2e Highly stressed electrospray of glycerol.  $V_{on} = 5200$  V. Distinct emission points are not observed any longer

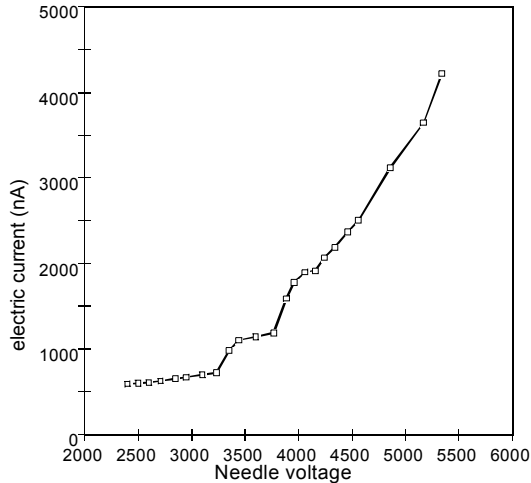


Figure 3 Electric current versus needle voltage for a glycerol solution. Additional cone-jets are generated in the needle rim as the voltage is increased. Formation of a new jet causes a current step and hence a thrust step.

As implied by Eq. [3], to achieve 20:1 thrust throttability the mass flow must be varied over similar interval. We achieve this by varying the propellant delivery pressure using a zeolite based feed system.<sup>12</sup> This approach was chosen over several alternatives because it contains no moving parts resulting in mechanically quiet system crucial for DRS type mission.

A combination of NMP/ST7-DRS mission requirements and self imposed requirements resulted in the specifications shown in Table 1. Some of the requirements, such as the total system mass and items 8 through 11 are not applicable to the first prototype laboratory system. As such they represent goals rather than requirements and a look ahead at what is likely to be needed in a more mature system. As will be discussed in subsequent sections most of the goals were met and some were exceeded.

Table 1 NMP Micro Newton Thruster Specifications and Requirements

#	Item	Specification	Comment
1	Thrust	1-20 $\mu\text{N}$	Smoothly variable between end point values within 0.1 $\mu\text{N}$
2	Thrust controllability/ resolution	0.1 $\mu\text{N}$	Must be within $\pm 0.1 \mu\text{N}$ from set point
3	Thrust noise	0.1 $\mu\text{N}$ RMS 10 - 1000 sec	Stable over given period
4	Specific impulse	$\geq 500$ sec	May vary depending on thrust
5	System mass	$< 2$ kg	Not applicable to breadboard
6	Total system power	$< 10$ W	Includes PPU
7	Total operating time	$\geq 1000$ hours	
8	Thrust slew rate	TBD $\mu\text{N}/\text{sec}$	
9	System efficiency/ thermal load on s/c	$>$ TBD	Maximize efficiency to minimize thermal loads on spacecraft. This is especially important to power processing efficiency which will dominate power losses.
10	Beam quality/ divergence	$<$ TBD degrees	Minimize beam spreading and slowly moving charged particles to avoid s/c contamination
11	Mechanical noise	$<$ TBD	Avoid moving parts at least during data taking

### 3.0 SYSTEM DESCRIPTION

The system schematic is shown in Figure 4. Photographs of the system as delivered to NASA

JPL are shown in Figure 5, Figure 6 and Figure 7. The system consists of the thruster, field emission neutralizer, PPU, propellant storage and feed system and two diagnostic pressure transducers not planned

for subsequent models. The system is controlled via National Instruments I/O card and LabView software commanding the thruster PPU from a conventional PC. In broad terms the system functions as follows.

1. CO<sub>2</sub> gas is desorbed from zeolite crystals by heating which pressurizes the propellant stored in stainless steel bellows.
2. Thruster extractor and accelerator voltages are applied.
3. Micro latching valve opens allowing propellant flow to the thruster.
4. Neutralizer emits electrons to match the emitted ion beam current.

Thruster off command closes propellant valve, turns off zeolite heater and removes voltages from

extractor and accelerator grids. The zeolite chamber is cooled by radiation and heat sinking into the surrounding structure. CO<sub>2</sub> is then adsorbed into the zeolite crystals in cyclical process that can be repeated indefinitely. Thrust is varied by adjusting accelerator voltage and mass flow rate via CO<sub>2</sub> pressure by zeolite temperature adjustments.

The whole system is enclosed in an aluminum housing measuring 5 x 5 x 9 in. (see Figure 7) and weighs slightly about 2.5 kg. There is much room for improvement given that this is the first laboratory prototype. The power consumption under steady state conditions is typically less than 6 Watts and a maximum of 4 W is used by the zeolite heater.

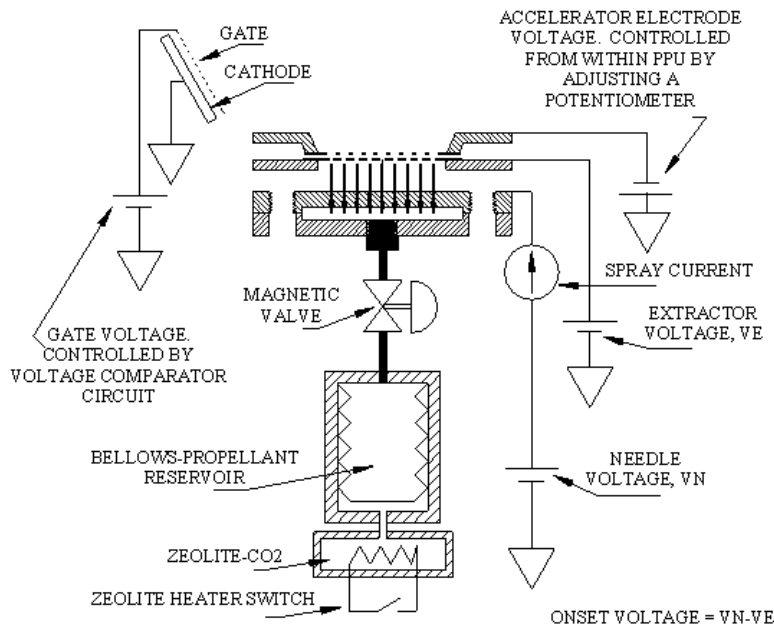


Figure 4 Schematic of the colloid thruster system.

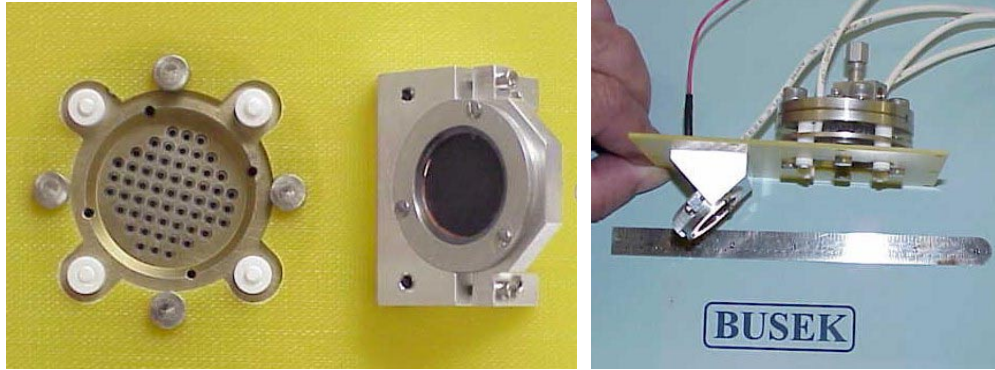


Figure 5 20  $\mu$ N colloid thruster and carbon nanotube (CNT) field emission (FE) neutralizer mounted on a common dielectric base.

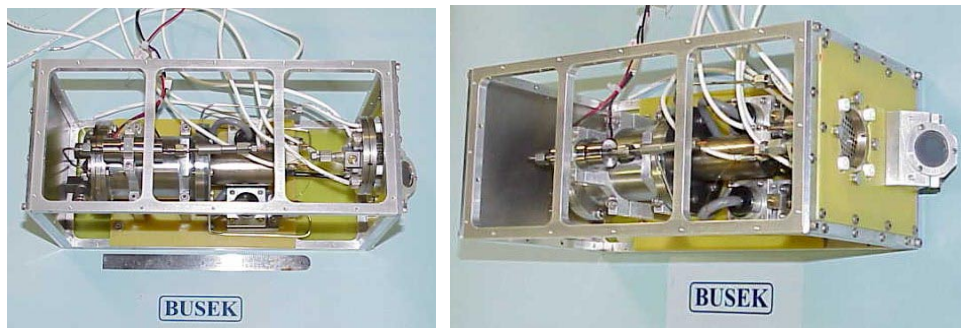


Figure 6 The 20  $\mu$ N colloid thruster system during the thruster, neutralizer and feed system integration



Figure 7 Assembled 20  $\mu$ N thruster system. Electron screen on the top allows rapid pump out. The PPU is inside the solid aluminum frame mounted on the side of the system housing and the thruster with neutralizer are mounted on a dielectric plate. Power and control signals are supplied via the 15 pin D type connector on the back side of the PPU frame

#### 4.0 DESCRIPTION OF COMPONENTS

##### 4.1 Colloid Thruster

A photograph of the thruster components is shown in Figure 8 and its cross-section is shown in Figure

9. The thruster was conveniently fabricated using 2-in. conflat flanges. An array of 57 stainless needles brazed into the emitter plate is mounted over the propellant cavity. The needles are approximately 1 cm long and have an OD of 180  $\mu$ m and an effective ID of 30 $\mu$ m. Aligned with the needles are the stainless steel extractor and accelerator grids

separated by ceramic spacers. Further details can be found in Ref. 13.

As will be discussed in subsequent sections the thruster can deliver broadly adjustable thrust depending on the propellant and its electrical conductivity. With a small beam deceleration it can deliver 1 to 20  $\mu\text{N}$  and demonstrated 20 to about 200  $\mu\text{N}$  using formamide with conductivity of 0.5 S/m.



Figure 8 Colloid thruster components conveniently fabricated from standard ConFlat flange.

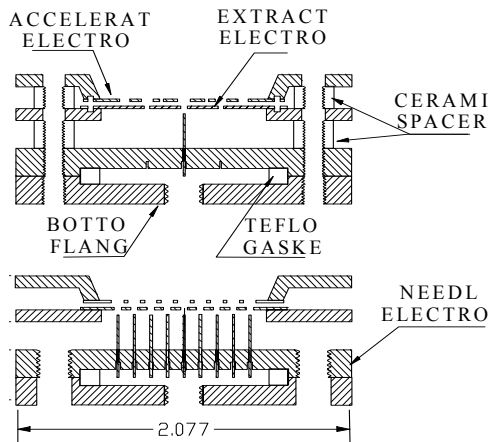


Figure 9 Colloid Thruster Cross-section

#### 4.2 Neutralizer

A field emission cathode based on carbon nanotubes was used as a neutralizer. A photograph shown in Figure 10 identifies the major components. In-house grown multi-wall carbon nanotubes are deposited on the emitter substrate which is electrically isolated from the base. A high porosity (55%)gate is placed

over the emitter and is at the potential of the cathode mounting base.

At approximately 250 V gate voltage the cathode delivers net of 50  $\mu\text{A}$  and a total of about 100  $\mu\text{A}$ . This exceeds the nominal ion beam current by a factor of 2. Similar cathodes were tested to 15 mA at up to 800 V gate voltage for short duration and one cathode was tested for 300 hours at 1 mA.

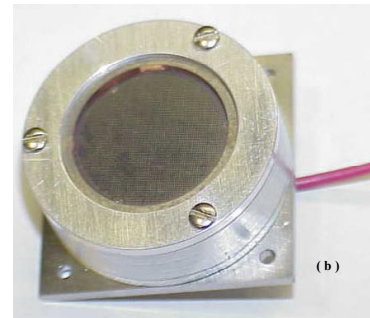
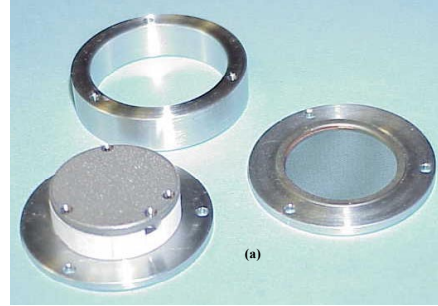


Figure 10 Carbon nanotube field emission neutralizer (a) Components, (b) Assembled neutralizer. The base dimension is approximately 3x3 cm.

#### 4.3 Power Processing Unit

Figure 11 shows the top view of the PPU implementation. While building this prototype, we decided to use standard sockets and surface pins to affix the electronic components whenever possible. This was mainly motivated by the possible eventuality of having to implement minor modifications after testing the PPU. A more advanced design will have the electronic components directly mounted on the board surface.

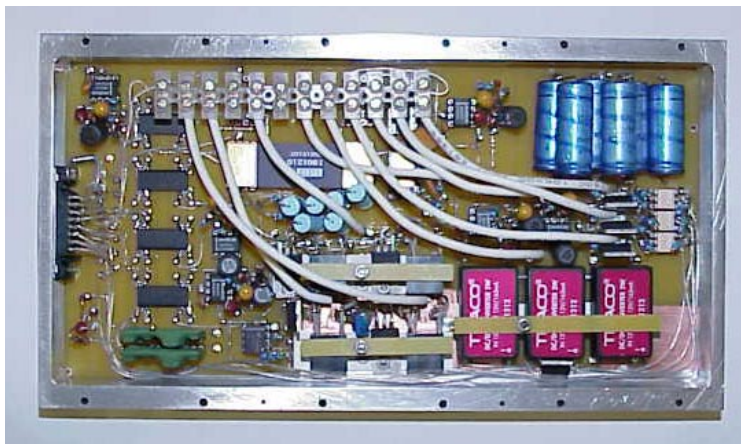


Figure 11 Top view of PPU prototype

Figure 11 reveals the major components which include: (1) EMCO converters to power the extractor, accelerator and the FE cathode gate, (2) TRACO converters which power the zeolite heater (a max of 4 W) and consume a major portion of the system power, (3) isolation amplifiers used primarily for interfacing with external inputs, (4) set of capacitors to drive the microlatching valve. All power and commands are supplied via 15 pin D connector.

The converters, specially the TRACOs, seem to slightly outgas. Thus, when the background pressure is approximately 10 m torr, the delivery of a high voltage by the EMCO HV converter is not possible (probably there is a minute discharge within the TRACO converters). However, the PPU operates correctly at a lower background pressure, e.g.  $10^{-5}$  torr.

The LabView program written to control the PPU is rather elementary. No strategies for automatic control have been implemented. The operator has access to all functions except for the automatic beam neutralization.

#### 4.4 Propellant Storage and Feed System

Schematic of the propellant storage and feed system is shown in Figure 12. It consists of a zeolite chamber that generates variable pressure  $\text{CO}_2$ ,

bellows chamber where the propellant is stored, micro latching valve and two optional pressure transducers employed here for diagnostic purposes. A capillary connects the feed system with the thruster and generates sufficient backpressure on the system. All propellant wetted components with the exception of elastomer seals that are necessary in a laboratory system are made of stainless steel.

The peak propellant pressure is dictated by the maximum flow rate and flow rate resolution with enough margin to account for the force to compress the bellows to its maximum extend. The maximum design flow rate is  $Q_{\max} \cong 3 \times 10^{-4}$  ml/min. To resolve 0.1  $\mu\text{N}$  implies flow rate resolution =  $Q_{\max}/20\mu\text{N}/0.1\mu\text{N} = 1.5 \times 10^{-6}$  ml/min. At  $Q_{\max}$  the propellant pressure drop is 178 torr and accounting for a margin in viscosity the max propellant pressure was selected to be 400 torr. The max  $\text{CO}_2$  pressure then must be 400 torr plus the pressure to achieve maximum bellows compression at the end of mission (approximately 450 torr). The bellows has a useful volume of 41 ml yielding about 3000 hours of operation with the present thruster.

Zeolites<sup>13</sup> are widely used in the petrochemical industry for preferential adsorption of certain gases. The process of adsorption and desorption can be repeated theoretically infinite number of times by lowering or increasing the zeolite temperature.

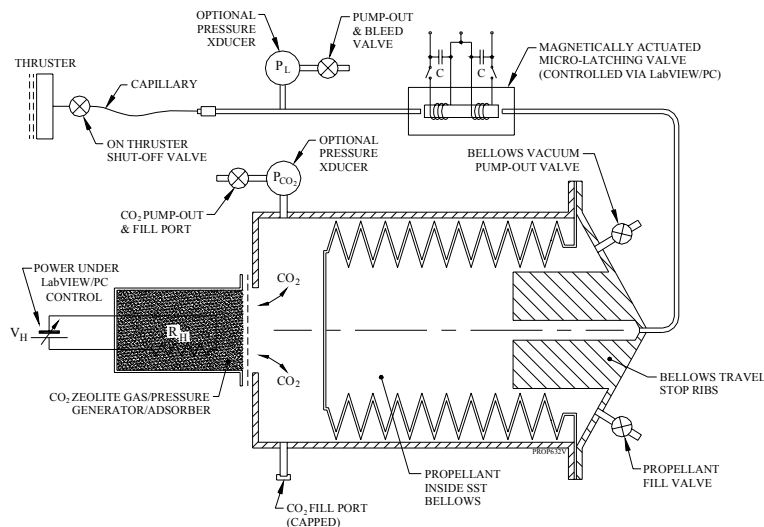


Figure 12 Schematic of the Propellant Storage and Feed System

While zeolites are most efficient in adsorbing hydrogen or hydrogen bearing molecules we selected to work with CO<sub>2</sub> as a benign, nontoxic, nonflammable gas. The repetitively measured zeolite mass gain, equal to the adsorbed CO<sub>2</sub> mass, ranged between 11.18 to 11.63% with an average of 11.48%.

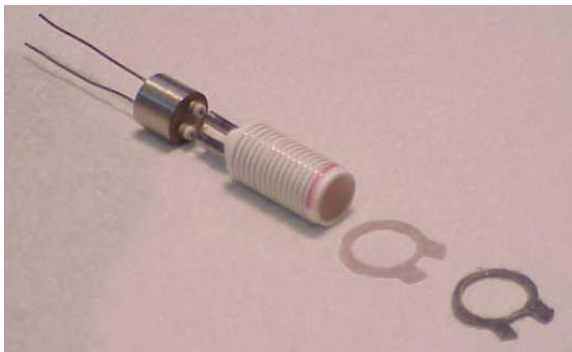


Figure 13 Photograph of the Zeolite Heater Prior to its Installation/Welding into the Zeolite Chamber

The total C<sub>2</sub>O loaded zeolite mass was 14.7 grams, which includes 1.5 grams of CO<sub>2</sub>. This mass of CO<sub>2</sub> can pressurize a volume of approximately 814 ml to 760 torr at room temperature. Thus zeolite chamber which contains the heater shown in Figure 13 is about order of magnitude larger than it has to be and can be used for systems that contain as much as 500 ml of propellant. We designed this oversized zeolite chamber to ensure that small CO<sub>2</sub> leaks while in vacuum, do not disable the feed system (this will not

be necessary with fully welded system with no O-rings) and to avoid working with very small heater dimensions.

The dynamic aspects of pressure generation is essentially dictated by the available heater power (to increase the pressure) and by heat sinking of the assembly to reduce the CO<sub>2</sub> pressure. As was shown by Shelton et al<sup>12</sup> the dynamics of the system also depends on the compression of the bellows. Because of our stringent flow control requirements, that mandate 1 torr pressure resolution, we must control the zeolite temperature to within 0.1° C. We plan in future systems to have a zeolite heater under closed loop feedback control by the colloid beam current which is proportional to the propellant mass flow. Commanded thrust corresponds to some beam current which in turn will control the heater power.

### Latching Valve

To minimize power consumption the feed system requires a latching valve. MEMs type micro valves<sup>14</sup> are generally made for gases, their behavior with conductive liquids at high voltage is not known and would require extensive investigation. Small commercial latching valves have significant dead volume (promoting bubble formation and trapping bubbles) and are very costly. Because of these reasons we decided to design and construct the latching valve shown in Figure 14. It has two

electromagnetic coils, one to close the valve by moving the armature with a small O-ring against its seat and one to open it. To hold the armature in position (valve closed or opened) permanent magnets are used. The valve is driven by discharging a capacitor (0.9 mF) through the coils with initial capacitor voltage of 28 Volts supplied by the PPU.

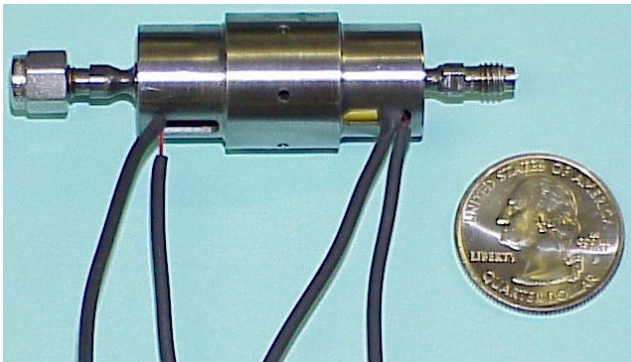


Figure 14 Photograph of a colloid thruster latching micro valve.

### Propellant Loading

As we experienced during our investigation a microbubble inside the liquid at atmosphere pressure (perhaps liberated in contact with the internal surface of the feed system) can generate thousands of large bubbles at  $10^{-5}$  torr. To achieve bubble free operation a special propellant loading technique was

developed. The propellant loading and feed system test apparatus is shown schematically in Figure 15. All propellant wetted components were located in vacuum, inside a Pyrex bell jar to permit visual observation.

The propellant container (most of the time we worked with TBP or formamide) was evacuated along with the zeolite chamber and the bellows via the various valves outside of the bell jar. This provided the initial liquid outgassing. The bell jar pressure of  $10^{-6}$  torr was typical, pumping over night. The propellant container was then pressurized to a few torr with  $\text{CO}_2$  pushing the propellant into the bellows and through the micro/latching valve, flow meter, and capillary into the indicated test vial. Then the propellant container was evacuated and  $\text{CO}_2$  was introduced into the zeolite chamber expelling the liquid back into the propellant container. This back and forth flushing process was repeated several times each time liberating decreasing number of bubbles (visible through the transparent container and vials). When no more bubbles were observed, the zeolite chamber was filled to about 40 torr (zero propellant flow pressure when connected to the thruster) and allowed to stabilize as determined by monitoring the  $\text{CO}_2$  pressure and the zeolite temperature via the indicate thermocouple.

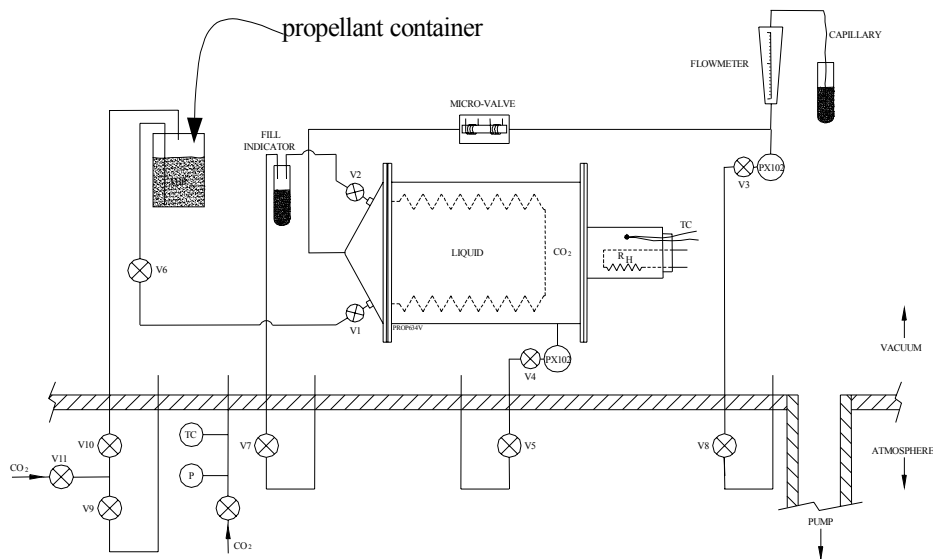


Figure 15 In-vacuum System Fueling Schematic. The Same Set-up with all Shut-off Valves Closed (V1, V2, V3, V4), was Used for Testing of the Feed System.

## 5.0 COMPONENT AND SYSTEM TESTING

### 5.1 Thruster Testing and Performance

The thruster described in Section 4 was tested using a formamide propellant with a measured electrical conductivity  $k=0.5$  S/m. Details of the experimental arrangement are given in companion paper<sup>15</sup>. The flow rate was varied using the baseline technique of variable propellant reservoir pressure and by varying the extractor voltage. Thrust and mass flow were measured using a time of flight spectroscopy<sup>15,1</sup>.

Representative thrust data are presented in Figure 16. The thrust varied between approximately 20 to 190  $\mu\text{N}$  and maximum  $I_{sp}$  was 400 sec. Lower than intended propellant conductivity resulted in slightly lower  $I_{sp}$  and much higher thrust than the target of 500 sec and 1 to 20  $\mu\text{N}$ . Further testing with higher conductivity propellant (nominally 1.5 S/m) and higher voltage power supplies is planned.

While the baseline flow rate throttling technique is the propellant reservoir pressure variation, Figure 16 shows that extraction by varying the extractor voltage ( $V_{ON}$ ) over a significant range (4:1) can be accomplished. This technique, used by FEETs<sup>2,3</sup>, is not expected to simultaneously satisfy 20:1 throttability and trust stability requirements because it leads to multi-cone jets (See Figure 2) and associated stepwise changes in thrust discussed in Section 2.

### 5.2 Beam Neutralization with FE Cathode

The thruster, the FE cathode and the PPU described in previous sections were tested together using the arrangement shown in Figure 17. Due to the facility geometrical constraints the FE cathode as placed about 5 cm downstream of the thruster (unlike the final, as shipped, arrangement shown in Figure 5, 6 and 7).

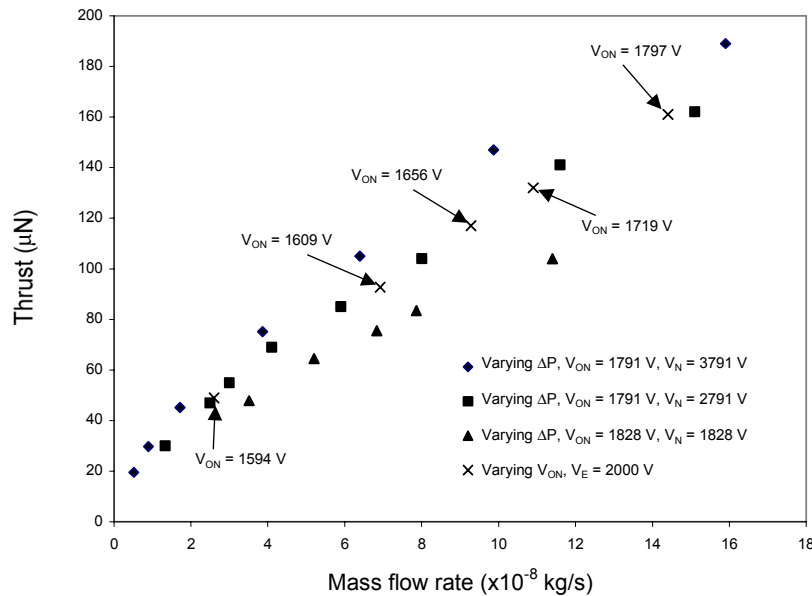


Figure 16 Thrust versus mass flow rate for the electro spray beams of a formamide solution  $K = 0.50$  S/m. The figure presents data for both “pressure controlled  $\dot{m}$ ” (three first series, taken at different acceleration voltages), and “voltage controlled  $\dot{m}$ ” (last data series) strategies

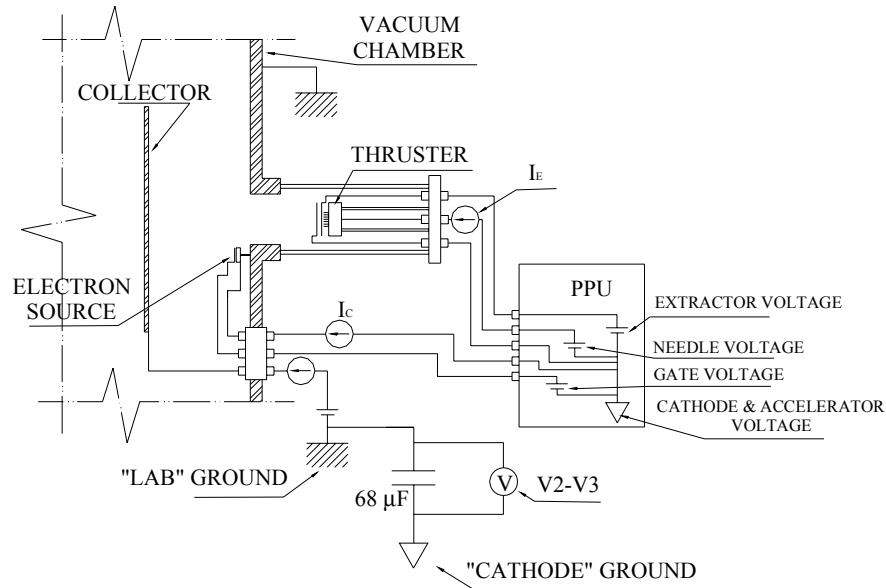


Figure 17 Schematics of the experimental setup used to test the neutralization of the electro spray beam

Since this was the first time an FE cathode was used to neutralize positive EP beam, it was decided to measure both the electron current and the beam current independently to confirm that current matching occurs. Current matching does not guarantee effective beam neutralization but does guarantee that the spacecraft will not be charged. Unlike conventional hollow cathode neutralizers that automatically deliver the matching electron current, the FE cathode gate voltage must be continuously adjusted to achieve matching. A special circuit built into PPU was used to vary the gate voltage depending on the voltage  $V_2 - V_3$ , across the  $68 \mu\text{F}$  capacitor shown in Figure 17. This voltage is equivalent to a voltage across a back-to-back zener diode that connects conventional ion or Hall thruster cathodes to spacecraft ground. When the  $V_2 - V_3$  exceeded  $-6.9 \text{ V}$  the EMCO converter raised the gate voltage for the cathode to deliver more current. The typical result is presented in Figure 18. In this figure  $I_{\text{beam}}$  is labeled as  $I_E$  and is approximately  $20 \mu\text{A}$ . When  $V_2 - V_3$  reaches the preset voltage ( $-6.9 \text{ Volts}$ ) the cathode delivers approximately  $40 \mu\text{A}$  with about 50% of it going to the cathode gate. A companion paper<sup>14, Error! Bookmark not defined.</sup> gives further details.

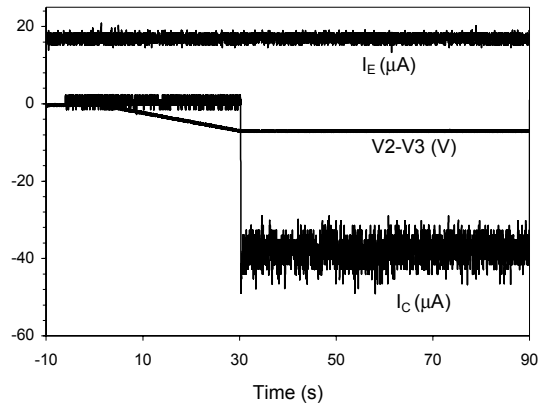


Figure 18 Evolution of the voltage difference between “cathode” and “lab” grounds, and the electro spray and cathode currents as a function time. Continuous electron emission is used to neutralize the electro spray beam

### 5.3 Feed System Testing

Typical desorption/adsorption curves for CO<sub>2</sub> in 4A type zeolite is shown in Figure 19. Starting at about 40 torr, the CO<sub>2</sub> pressure was increased to 1200 torr (a pressure ratio of 30) over 60°C interval starting at room temperature. This confirms our earlier statements about excess capacity of the present zeolite chamber. The shallow  $dp/dT$  slope in the low pressure range indicates that to have 1 torr resolution will require approximately 0.1°C temperature control. Although readily achievable, we plan to control the pressure in the future by a feedback loop from the thruster beam current that by passes temperature measurement

A typical histogram of the CO<sub>2</sub> pressure and zeolite temperature measured with the system in vacuum is

shown in Figure 20. The system was configured as shown in Figure 15 with some tests performed while powered with the PPU. The propellant was expelled through the opened latching valve, flowmeter and capillary into a small vial. The procedure was to heat the zeolite at a constant input power until the temperature stabilized and then the power was increased. The starting CO<sub>2</sub> pressure was approximately 40 torr. From 0 to 76 minutes the power was 1.55 Watts, from 76 to 191 minutes the power was 2.22 Watts and from 191 to 225 minutes the power was 4.13 Watts, which approaches the maximum the PPU can deliver. The propellant pressure closely tracks the CO<sub>2</sub> pressure until significant bellows compression is required.

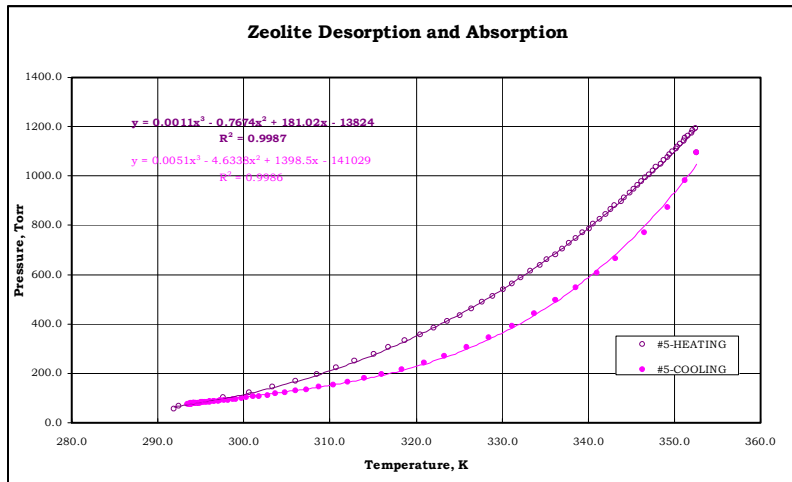


Figure 19 Typical Desorption and Adsorption Curves for CO<sub>2</sub> in Type 4A Zeolite Measured Using our Zeolite Chamber

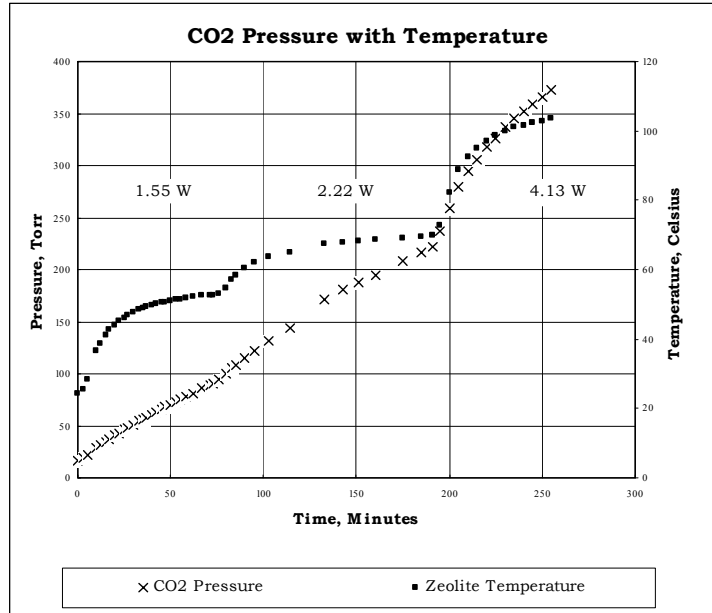


Figure 20 Typical Histogram of Zeolite Temperature and CO<sub>2</sub> Pressure Measured Using our Feed System

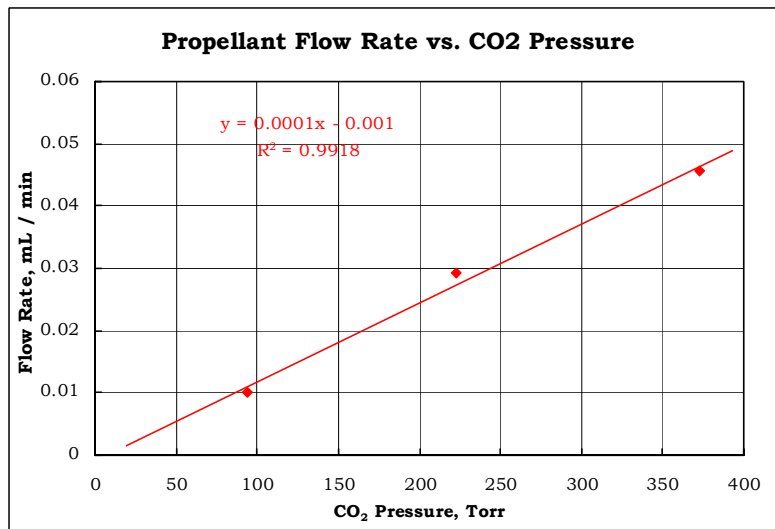


Figure 21 Propellant Flow Rate Versus CO<sub>2</sub> Pressure Measured with our Feed System. The Zero Intercept is at 22 torr which corresponds to the bellows precompression

The measured propellant flow rate plotted versus the CO<sub>2</sub> pressure in Figure 21 exceeded its specified maximum (0.0003 ml/min) by two orders of magnitude. This is due to two factors, the bellows was nearly full (no spring compression required) and the capillary at the exit of the feed system was sized for rapid testing (and pump out) in conjunction with a simple flowmeter (Gilmont Instruments F-2060) that is usable in vacuum. Testing the system in the range of flow rates from 0.0003 to 0.00001 ml/min

would have required tens of hours of testing so instead, we opted for demonstration of the required pressures. A simple change in capillary length or diameter will then produce the required flow rate.

As anticipated, the relationship between the flow rate and pressure in Figure 21, is linear and the zero flow intercept occurs at about 22 torr which is dictated by the level of bellows precompression. The predicted value was  $p_b=27$  torr.

As Figure 20 and Figure 21 show the CO<sub>2</sub> pressure and the propellant pressure approaches 400 torr. Similar pressures will be required when employing the much smaller capillary to achieve adequate flow resolution. Taking the average slope of the CO<sub>2</sub> pressure ( $\cong$  propellant pressure) versus time at the highest power (4.13 W in Figure 20) it is evident that  $dp/dt$  is about 250 torr/hour. To achieve a target of 360 torr/hour would require an improved thermal design which is certainly possible and possibly a compromise between lower flow resolution and higher heater input power.

#### 5.4 Integrated System Test

The integrated thruster-neutralizer-PPU test was successfully carried out as described in previous sections. The integrated feed system with PPU test was also successfully completed as described above, with the PPU operating the latching micro valve and powering the zeolite heater while in vacuum. The fully integrated system test with the thruster, neutralizer, PPU and feed system all housed in its common enclosure, was not carried out due to the system delivery deadline. We have no reason to believe that this test would not be successful.

### 6.0 CONCLUSIONS

A complete laboratory colloid thruster system was designed, constructed, tested and delivered to NASA JPL. The laboratory system containing the thruster, neutralizer, PPU and the propellant feed/storage system is housed in a single rectangular enclosure measuring 9x5x5 inches and weighs approximately 2.5 kg. Neither the mass nor the volume is optimized and can be substantially reduced. The typical power consumption is approximately 6W. The zeolite heater consumes a maximum of 4 W.

The 1 to 20  $\mu$ N thrust range was not demonstrated, instead we demonstrated 20 to 189  $\mu$ N with maximum Isp of 400 sec. Demonstration of the lower thrust range and higher Isp is planned using a higher conductivity propellant. This performance scaling with increasing propellant conductivity was demonstrated previously with a single needle thruster<sup>1</sup>. Thrust stability better than 0.01  $\mu$ N with a

single needle thruster on a thrust stand is reported in companion paper<sup>15</sup> and there is no reason to expect that 0.1  $\mu$ N with the present multineedle thruster cannot be achieved.

The PPU and the LabView based control system performed as designed and its implementation exceeded the program requirements. The PPU powered from a single 12 VDC source contains all the circuitry to power the thruster, neutralizer and feed system and has a bi-directional interface with the LabView hosting computer.

The first demonstration of a field emission neutralizer was completely successful. Two neutralization techniques under automatic control of the PPU were demonstrated. The existing CNTFE cathode is capable to neutralize much larger thruster.

The zeolite based CO<sub>2</sub> pressure generator worked as designed and it too can serve much larger system. The bellows system storing 40 ml of propellant is adequate for testing up to about 3000 hours. The system worked well once the proper system fueling method was established. The magnetically actuated small latching valve worked as designed.

The integrated thruster-neutralizer-PPU subsystem and the propellant feed system-PPU subsystem were successfully tested. The completely integrated system test is planned. A duplicate system is in construction and will be delivered to NASA GRC as a part of the ongoing SBIR effort. We plan to test the completely integrated system before its delivery and demonstrate 1 to 20  $\mu$ N thrust and 0.1  $\mu$ N thrust stability using the newly available micro Newton thrust stand<sup>16</sup>.

#### Acknowledgements

Three programs contributed to the work presented herein including the NASA JPL New Millennium Micro Newton Thruster Program led by Dr. J. Blandino and Dr. W. Folkner, NASA GRC SBIR Colloid Thruster Program led by Dr. J. Sovey and Carbon Nanotube Field Emission Cathode Program led by Mr. C. Sarmiento of NASA GRC and sponsored by BMDO SBIR office under Mr. J. Bond. The authors would like to thank all of them for the opportunity to work on this exciting technology.

- 1 Gamero-Castaño, M. and Hruby, V., "Electrospray as a source of nanoparticles for efficient colloid thrusters" (2000). *Journal of Propulsion and Power* 7, 977-987 (2001).
- 2 A. Genovese, et al., "Indium FEEP Microthruster: Experimental Characterization in the 1-100  $\mu$ N Range," AIAA 2001-3788, *37<sup>th</sup> Joint Propulsion Conference*, Salt Lake City, UT, July 2001.
- 3 M. Tajmar, et al., "Indium FEEP Thruster Beam Diagnostics, analysis and Simulation," AIAA 2001-3790, *37<sup>th</sup> Joint Propulsion Conference*, Salt Lake City, UT, July 2001.
- 4 Provided by Dr. William Folkner/JPL.
- 5 Kidd, P.W. and Shelton, H., "Life Test (4350 hrs.) of an advanced colloid thruster module", Paper AIAA 73-1078, AIAA 10th Electric Propulsion Conf., Lake Tahoe, NV, 1973
- 6 Huberman, M.N. and Rosen, S.G., "Advanced high-thrust colloid sources", *J. of Spacecraft*, Vol. 11, no. 7, July 1974, pp. 475-480.
- 7 Fernandez de la Mora, J. and Loscertales, J.G., "The current emitted by highly conducting Taylor Cones". *J. Fluid Mech.*, vol. 260, pp. 155-184 (1994).
- 8 Fenn, J. B., Mann, M., Meng, C. K., Wong, S.K. & Whitehouse, C. "Electrospray Ionization for Mass Spectrometry of Large Biomolecules," *Science*, 246, 64-71, 1989.
- 9 NASA Glenn Research Center — "Colloid Thruster for Micro and Nano Satellites," NASA Contract No. NAS 2-99014, 1998.
- 10 M. Martinez-Sanchez, J. Fernández de la Mora, V. Hruby, M. Gamero-Castaño & V. Khayms., "Research on Colloid Thrusters," *26th International Electric Propulsion Conference*, Kitakyushu, Japan, October 1999.
- 11 "A Phase-A Study of the Disturbance Reduction System proposed for New Millennium Space Technology 5," Jet Propulsion Laboratory, California Institute of Technology, July 15, 1999.
- 12 Shelton, H. et al, *Charged Droplet Electrostatic Thruster Systems*, AFAPL-TR-70-31, AFEPL, Wright-Patterson Air Force Base, OH, June 1970.
- 13 Breck, Donald W., **Zeolite Molecular Sieves**, John Wiley & Sons, New York
- 14 Mueller, Juergen, "Review and Applicability Assessment of MEMS-Based Microvalve Technologies for Microspacecraft Propulsion," Micci, Michael M. and Ketsdever, Andrew D., **Micropropulsion for Small Spacecraft**, pg. 449
- 15 Gamero-Castaño, M., Hruby, V., "Characterization of a Colloid Thruster Performing in the micro-Newton Thrust Range," IEPC-01-282, *27<sup>th</sup> International Electric Propulsion Conference*, Pasadena, CA, October 2001.
- 16 Gamero-Castaño, M., Hruby, V., and Martinez-Sanchez, M., "A Torsional Balance that Resolves sub-micro-Newton Forces," IEPC-01-235, *27<sup>th</sup>*

---

*International Electric Propulsion Conference*, Pasadena, CA, October 2001.